

45th AIAA Aerospace Sciences Meeting and Exhibit
Jan 8-11, 2007, Reno, Nevada

Special Session – Towards A Silent Aircraft

Airframe Design for “Silent Aircraft”

J. I. Hileman^{*}, Z. S. Spakovszky[†], M. Drela[‡]

Gas Turbine Laboratory, Massachusetts Institute of Technology, Cambridge, MA, 02139

M. A. Sargeant[§]

Cambridge University, Cambridge CB2 1PZ, UK

The noise goal of the Silent Aircraft Initiative, a collaborative effort between industry, academia and government agencies led by Cambridge University and MIT, demands an airframe design with noise as a prime design variable. This poses a number of design challenges and the necessary design philosophy inherently cuts across multiple disciplines involving aerodynamics, structures, acoustics, mission analysis and operations, and dynamics and control. This paper discusses a novel design methodology synthesizing first principles analysis and high-fidelity simulations, and presents the conceptual design of an aircraft with a calculated noise level of 62 dBA at the airport perimeter. This is near the background noise in a well populated area, making the aircraft imperceptible to the human ear on takeoff and landing. The all-lifting airframe of the conceptual aircraft design also has the potential for a reduced fuel burn of 124 passenger-miles per gallon, a 25% improvement compared to existing commercial aircraft. A key enabling technology in this conceptual design is the aerodynamic shaping of the airframe centerbody which is the main focus of this paper. Design requirements and challenges are identified and the resulting aerodynamic design is discussed in depth. The paper concludes with suggestions for continued research on enabling technologies for quiet commercial aircraft.

I. Introduction

THE heretofore unasked technical question what an aircraft would look like that had noise as one of the primary design variables calls for a “clean-sheet” approach and a design philosophy aimed at a step change in noise reduction. While the aircraft noise during take-off is dominated by the turbulent mixing noise of the high-speed jet, it is the airframe that creates most of the noise during approach and landing. To reduce the aircraft noise below the background noise level of a well populated area, it is clear that the airframe and the propulsion system must be highly integrated¹ and that the airframe design must consider aircraft operations for slow and steep climb-outs and approaches to the airfield.^{2,3} Furthermore, the undercarriage must be simple and faired, and high-lift and drag must be generated quietly. A candidate configuration with the above characteristics is the Silent Aircraft eXperimental design SAX-40, as shown in Figure 1. The conceptual aircraft design uses a blended-wing-body type airframe^{4,5} with an embedded, boundary layer ingesting, distributed propulsion system, discussed in depth in a companion paper.⁶ The details of the engine design can be found in Hall and Crichton^{7,8} and de la Rosa Blanca et al.⁹ The engine inlets are mounted above the airframe to provide shielding of forward radiating engine noise¹⁰ while the embedding of the propulsion system in the centerbody enables the use of extensive acoustic liners.¹¹

As depicted in Figure 1, the airframe design incorporates a number of technologies necessary to achieve the step change in noise reduction. The all-lifting, smooth airframe was designed for advanced low speed capability to reduce noise and efficient cruise performance to improve fuel burn. The details of the aerodynamic design are the focus of this paper and are discussed at length. A simple and faired undercarriage in combination with reduced approach velocities mitigates the noise generated by unsteady flow structures around the landing gear and struts as discussed in Quayle et al.^{12,13} To achieve the low approach velocities, deployable drooped leading edges are used in combination with the advanced airframe design. The necessary drag for a quiet approach profile is generated via

^{*} Research Engineer, Department of Aeronautics and Astronautics, 77 Massachusetts Ave, Member AIAA.

[†] Associate Professor, Department of Aeronautics and Astronautics, 77 Massachusetts Ave, Member AIAA.

[‡] Professor, Department of Aeronautics and Astronautics, 77 Massachusetts Ave, Fellow AIAA.

[§] Ph.D. Student, Engineering Department, Trumpington Street, Member AIAA.

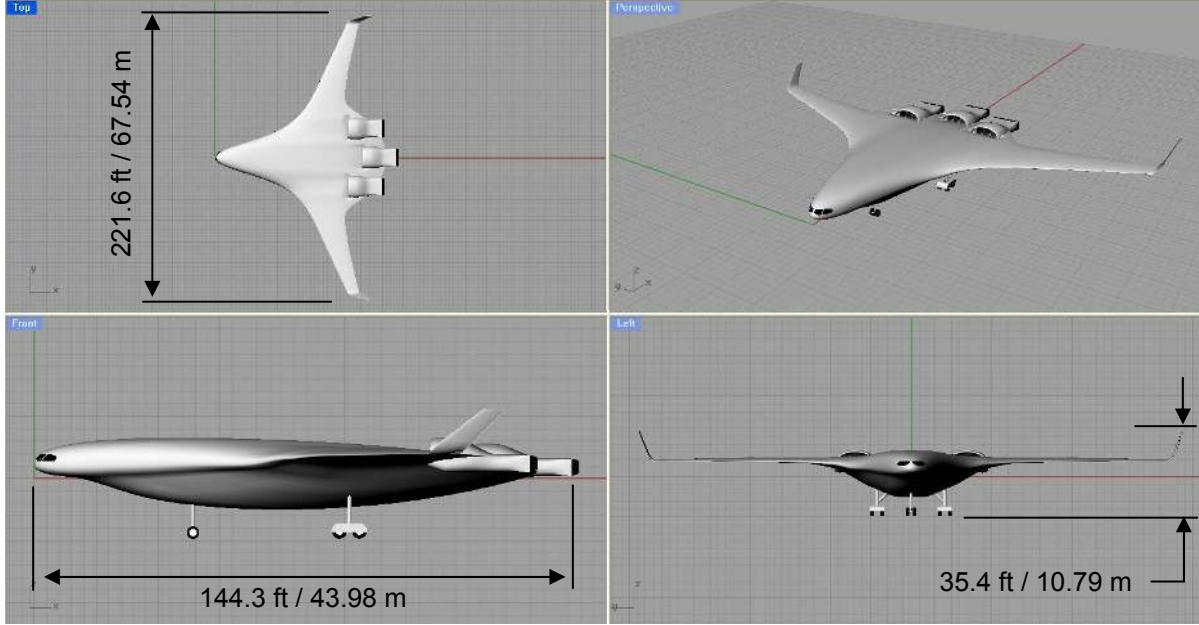


Figure 1. Silent Aircraft eXperimental design SAX-40.

increased levels of induced drag through an inefficient lift distribution over the all-lifting airframe during approach. This is achieved via a combination of upward deflected elevons and vectored thrust. Although not used on the conceptual aircraft design presented here, other quiet drag concepts were investigated which are potentially applicable for conventional aircraft configurations. For example the acoustic signature of perforated drag plates is reported in Sakaliyski et al.¹⁴ and a novel, quiet engine airbrake concept based on steady swirling flow to generate pressure drag is discussed in Shah et al.¹⁵ The airframe trailing edges are acoustically treated by deploying brushes to reduce the airfoil self-noise. This concept is similar to the quiet flight of the owl where the feathers are used to reduce the flow noise of the wings as reported by Lilley.⁶ A noise reduction of about 4 dB was experimentally demonstrated by Herr and Dobrzynski¹⁷ using trailing edge brushes on a scale model aircraft wing.

The present paper focuses on the detailed airframe design for a step change in noise reduction and improved fuel burn. More specifically, the objectives are to (1) introduce a newly developed quasi-three dimensional aerodynamic airframe design methodology based on the above ideas and concepts, (2) validate the methodology using three-dimensional Navier-Stokes simulations of a candidate airframe design, and (3) define and optimize a conceptual aircraft design for low noise and improved fuel efficiency by combining the methodology with noise assessment tools. The resulting conceptual aircraft design, SAX-40, yields a calculated noise level at the airport perimeter of 63 dBA and has the potential for a fuel burn of 124 passenger-miles per gallon, a 25% improvement compared to existing commercial aircraft. Given the high risk of the technologies used, SAX-40 meets the objectives of a “silent” and fuel efficient conceptual aircraft design.

The paper is organized as follows. The design requirements and challenges for a “silent” and fuel efficient aircraft are discussed first. Next, the key features of the aerodynamic airframe design are outlined, elucidating how a step change in noise reduction and enhanced aerodynamic performance are achieved. The evolution of the airframe design along with the characteristics of three generations of designs is briefly summarized. The airframe design methodology and framework used in the last generation of designs is then described in detail. Next, the established aerodynamic design framework is validated using a three-dimensional Navier-Stokes calculation of a candidate airframe design. The framework is then used to optimize for low noise and improved fuel efficiency, and the resulting design, SAX-40, is discussed in detail. Last, the findings and conclusions are summarized and an outlook on future work is given.

II. Key Challenges and Enabling Concepts

A key airframe design requirement necessary to achieve the approach noise goal is the capability of the aircraft to fly a slow approach profile. The sound pressure levels of the airframe noise sources scale with $1/r^2$ and u^n where r

is the distance between source and observer, and u is the approach velocity. The exponent n is 5 or 6 depending on whether the noise stems from scattering of turbulent structures near edges or acoustic dipoles. The scaling law thus suggests that the noise at the observer location can be reduced by using a slow approach profile and by landing further into the runway^{3,18} to keep the aircraft at higher altitude when crossing the airport perimeter. This requires a low stall speed of the airframe and correspondingly increased amounts of drag. The low approach speed determines the landing field length, which combined with the runway length, sets the threshold displacement. Although the conceptual design is strongly governed by noise considerations, fuel economy and emission levels must be competitive with next generation aircraft. This requirement raises the question whether trade-offs between noise and fuel burn need to be made and, if so, what the potential penalty for noise reduction is. The paper demonstrates that, by taking advantage of the all-lifting configuration and by aerodynamically shaping the airframe centerbody, *both* a reduction in noise *and* an improvement in fuel burn can be achieved.

A. Major Challenges

The above requirements introduce major design challenges. The first challenge is to achieve competitive cruise performance while maintaining effective low speed aerodynamic characteristics. For a given aircraft weight, either the area or the lift coefficient need to be increased during landing to reduce the approach velocity. This demands variable wing geometry such as for example conventional flaps and slats which are inherently noisy and must thus be avoided. Circulation control^{16,18} is one possible option to achieve enhanced high lift capability without a variable wing geometry but the impacts of weight and complexity of the flow control system on overall performance and cruise efficiency need yet to be assessed in detail. The idea adopted here is to avoid this complexity and to incorporate passive circulation control in the aerodynamic design of the all-lifting airframe by optimally shaping its centerbody.

In order to achieve the noise goal, the lifting surfaces must be smooth and the undercarriage needs to be simple and faired. This inherently reduces the drag on approach which poses another challenge in the design of a low noise aircraft. The drag required for a slow approach profile must be generated in quiet ways. The concept used here is to increase the induced drag by setting up an inefficient but relatively quiet lift distribution over the airframe during approach.

Another major challenge lies in trimming and rotating a tailless airframe such as the all-lifting configuration considered here. Pitch trim and static stability can be achieved without a tail but require reflexed airfoils on the centerbody.⁴ The major drawbacks thereof are a penalty in cruise performance and relatively large control surfaces and actuation power to facilitate rotation. As discussed next, aerodynamically shaping the leading edge region of the centerbody enables pitch trim and static stability without the use of reflexed airfoils or canards.

B. Key Airframe Design Feature

It is important to note that the holistic approach and the integrated system design of SAX-40 are crucial to achieve the noise goal and to improve fuel burn. In this, the all-lifting airframe incorporates a key design feature that distinguishes the conceptual aircraft design presented here from other blended-wing body type concepts. As depicted in Figure 1, the leading edge region of the centerbody is aerodynamically shaped and the all-lifting airframe is optimized to generate a lift distribution that (i) balances aerodynamic moments for pitch trim and provides a 5 to 10% static stability margin while avoiding a horizontal tail lifting surface and reflexed airfoils, (ii) achieves an elliptical span load on cruise yielding a 15% improvement in ML/D compared to current blended-wing body aircraft designs, and (iii) increases the induced drag on approach via elevon deflection and vectored thrust, reducing the stall speed by 28% compared to currently operating airframes.

The in-depth analysis of this advanced airframe design and the underlying aerodynamic characteristics are the subject of this paper and are discussed next.

III. Airframe Design Evolution

The SAX-40 aircraft design is the culmination of an iterative design process which, in retrospect, evolved from three major aircraft design generations. In each generation the assessment tools were further developed to improve fidelity and the redesigns were aimed at closing the gap between the estimated aircraft performance and the design goals. In conclusion of each of these major design steps, technical reviews were held with the Boeing Company and Rolls Royce plc. This section highlights the major characteristics and outcomes of the design evolution.



Figure 2: Three major generations of conceptual aircraft designs: SAX-12, SAX-20, and SAX-40.

A. First Generation SAX Design

The first generation of SAX designs utilized a modified version of Boeing's Multi-disciplinary Design Optimization code WingMOD^{4,19} where the objective function for the optimizer was focused on minimizing takeoff weight. This design process culminated in the SAX-12 planform,⁵ As shown in Figure 2 on the left, the configuration incorporates four boundary layer diverting Granta-252 engines.^{7,8} The cruise altitude, Mach number, range, and passenger capacity were held constant for SAX-12 and subsequent designs. The aircraft design was calculated to have an MTOW of 340,150 lb, a fuel burn of 88 passenger-miles per gallon (based on a passenger weight of 220 lbs), and maximum noise levels at the airport perimeter of 80 and 83 dBA during takeoff and approach, respectively.⁵ Considerable challenges remained before the noise goal could be achieved; chief among them was the lack of a methodology to optimize the airframe shape for low noise. Thus a clear need was the capability to define the three-dimensional geometry of the airframe and a novel airfoil stack. The SAX-12 planform shape, airfoil thickness distribution, minimum cabin size, rear spar location, and mission were carried over as starting points in the next generation of aircraft design. In addition, WingMOD was used to create the structure weight response-surface-model that was used throughout the design process.

B. Second Generation SAX Design

The focus of the second generation of SAX designs was the development and validation of a quasi-3D airframe design methodology with inverse design capabilities. A first version of this methodology was previously reported by the authors²⁰ and improvements will be discussed in Section IV. For the second generation of designs, this methodology was used to achieve a significant reduction in noise by reducing the stall speed. This resulted in aerodynamic shaping of the centerbody leading edge with supercritical profiles designed for the outer-wing sections. The design process started with SAX-15 and culminated in the SAX-29 planform, shown in Figure 2 in the center. This design incorporated a boundary layer ingesting, distributed propulsion system based on three engine clusters. Each engine cluster consisted of a single gas generator driving three fans. To assess the methodology and the effectiveness of the centerbody aerodynamics, a three-dimensional Navier Stokes calculation was carried out for the SAX-29 airframe at Boeing Phantom Works. The details of the analysis are presented in Section V. The quasi-3D design methodology was successfully validated such that the airfoil profiles and detailed centerbody shape of the SAX-29 design were used in subsequent airframe designs.

C. Third Generation SAX Design

The third and last generation of designs focused on further refinement of the aerodynamics and the weight models by taking full advantage of the optimization capability of the design methodology. A gradient based optimization of the outer wing shape was used to minimize a cost function combining approach noise and fuel burn as metrics. The outcome of the optimization culminated in the SAX-40 planform, shown in Figure 2 on the right and discussed at length in Section VI. Similar to the second generation SAX-29 design, SAX-40 incorporates three Granta-3401 boundary layer ingesting engine clusters. The distributed propulsion system consists of three gas generators and nine fans. Engine and transmission system design details can be found in de la Rosa Blanco et al.⁸ and the integration of the propulsion system into the airframe is discussed in Plas et al.⁶ The SAX-40 aircraft design was calculated to have an MTOW of 332,560 lb, a fuel burn of 124 passenger-miles per gallon (based on a passenger weight of 240 lbs), and maximum noise at the airport perimeter of 63 dBA.^{2,3}

D. Design Comparison

As the SAX design evolved, significant gains in ML/D were achieved and the approach velocity was reduced while increasing the planform area as tabulated in Figure 3. Most of the improvement in ML/D can be attributed to the aerodynamic shaping and cambering of the centerbody leading edge which enabled a nearly elliptical lift distribution. In addition, as shown in Figure 3, the optimization process increased the planform area, slightly unswept the wings and grew the span, yielding a reduction in stall speed. The full optimization of the three-dimensional airframe geometry demonstrates that a configuration with both lowered noise emission *and* improved fuel burn can be achieved. This was not clear prior to the optimization as it was hypothesized that cruise performance penalties would have to be incurred for reduced approach noise.²⁰

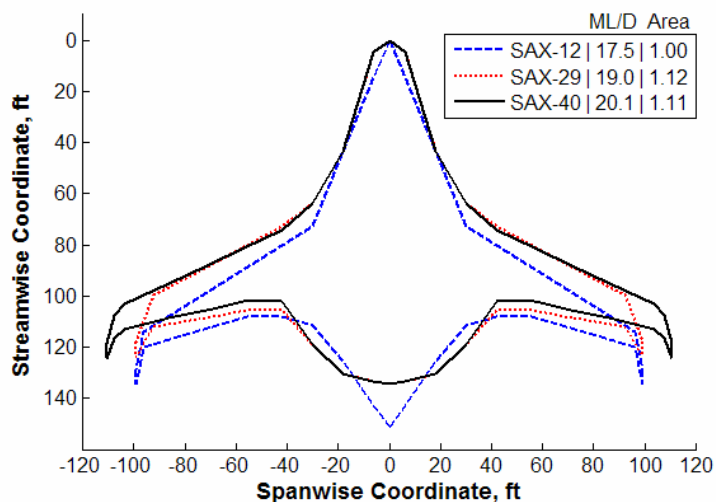


Figure 3: Evolution of SAX planform and aircraft performance.

IV. Technical Approach – Quasi-3D Design Methodology

The unconventional airframe configuration yields a highly three-dimensional aerodynamic design problem which requires a three-dimensional analysis to capture the centerbody aerodynamics. The involved computations are too costly to fully explore the design space with viscous three-dimensional calculations so a framework with a faster turnaround time but yet adequate fidelity was developed. Building on previous work by the authors, a quasi-3D design methodology was refined combining a two-dimensional vortex lattice method with sectional viscous airfoil analyses and empirical drag estimates of the three-dimensional centerbody, enabling rapid design iterations and optimization. At every major design change during this iterative process a fully three-dimensional flow assessment was conducted. A three-dimensional vortex panel method and Euler calculation of the entire airframe were carried out to assess the loading of the airfoils and shock strength obtained from the quasi-3D design methodology. To validate the overall framework and procedures, a three-dimensional Navier Stokes calculation was conducted and the results demonstrated good agreement with the established quasi-3D design methodology. An outline of the design methodology is given in this section and the details of the validation are discussed in Section V.

The quasi-3D design methodology, schematically shown in Figure 4, can be broken into three main parts, (i) airframe creation, (ii) cruise performance analysis, and (iii) low-speed performance analysis. The three-dimensional airframe shape is created from an airfoil profile stack and planform shape. This planform must enclose the spar box and is assessed over five mission points: takeoff rotation, takeoff climb-out, begin cruise, end cruise, and approach. The methodology iteratively estimates the aerodynamic performance using the procedure outlined previously by the authors. The design framework estimates stall and landing speed, landing field length, and elevon deflection / thrust vectoring requirements for pitch trim during approach and landing. During take-off, the elevon deflection / thrust vectoring requirements are assessed for rotation, and the aerodynamic performance is estimated during climb-out. This analysis guided the propulsion system design as described in more detail in Crichton et al.² and also provided an estimate for the airframe noise during take-off and approach.

The aerodynamic design framework discussed in the present paper differs from the previous version in a number of ways. The wing twist was defined over three segments with non-zero twist at the aircraft centerline, and the wave drag of the outer wings was estimated using MSES, a compressible, two-dimensional airfoil analysis tool. The trimmed stall speed of the aircraft was estimated by combining a two-dimensional vortex lattice approach (AVL) and a viscous airfoil analysis (XFoil). In this approach the aircraft angle of attack and elevator deflection for trim were iterated until the maximum airfoil sectional lift coefficient was reached.

To improve the assessment of aircraft weight, the following modifications to the weight models were implemented. The operating empty weight of the aircraft was estimated using an empirical model for the fixed

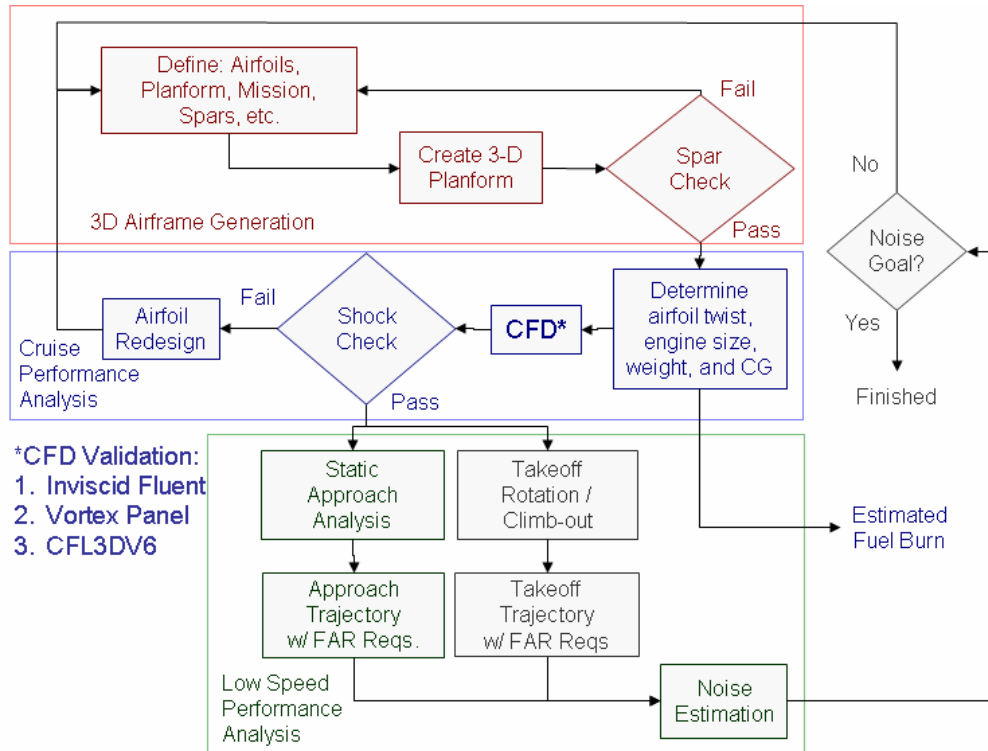


Figure 4: Quasi-3D design methodology used in the creation of the SAX-40 planform.

equipment and landing gear weights, a WingMOD based response surface model was used to compute the structures weight,²¹ and the propulsion system weight was quantified using the model described in de la Rosa Blanco et al.⁸ The structures weight model assumed a 10% improvement in composite material weight by 2025. The fuel weight was determined iteratively based on OEW and design payload using the calculated cruise ML/D and an assumed fuel burn of 2% of MTOW during climb. The center of gravity of the aircraft was estimated using the center of gravity of the systems, payload, fuel, propulsion system, and structure. Assuming a uniform density of the airframe materials, the center of gravity of the structure was determined based on the airframe center of volume. The landing gear was placed on the airframe such that rotation is assured and a tail-strike avoided. The detailed design of the undercarriage can be found in Quayle et al.¹² The aircraft dynamics during rotation, take-off and climb-out were assessed using aerodynamic performance parameters obtained from AVL and XFOIL. In addition, the aircraft dynamic response to gusts and go-around maneuvers was analyzed. A detailed discussion and results can be found in companion papers.^{5,22}

For the third generation of aircraft designs, constrained nonlinear optimization using sequential quadratic programming (SQP) was carried out to optimize the outer wing shape. The objective function was a linear combination of fuel burn and approach noise. The variables defining the outer wing shape included the leading edge sweep, wing chord at spanwise section 5 (spanwise location of 42.0 ft / 12.8 m), wing chord near the wing tip, and the outer wing span. Constraints were placed on the maximum angle of attack at the beginning of cruise (less than 3°), maximum leading edge loading (ΔC_p less than 1.0), minimum static margin at begin cruise (greater than 25 inches), minimum distance between elevator and wing spar (greater than 0.3 ft / 0.1 m), and maximum takeoff weight (less than 346,000 lb) to limit propulsion system growth. The optimization routine used multiple wing shapes as initial condition. In addition, the weightings of fuel burn and approach noise in the objective function were varied to yield a Pareto front of fuel burn versus approach noise from which the SAX-40 design was chosen.

V. Design Methodology Validation

The validation of the design methodology consisted of a comparison between a three-dimensional Navier Stokes solution and the results obtained from the quasi-3D design methodology involving an Euler solution, a vortex panel solution, and a vortex lattice solution. The primary objective was to assess the fidelity of the design methodology in

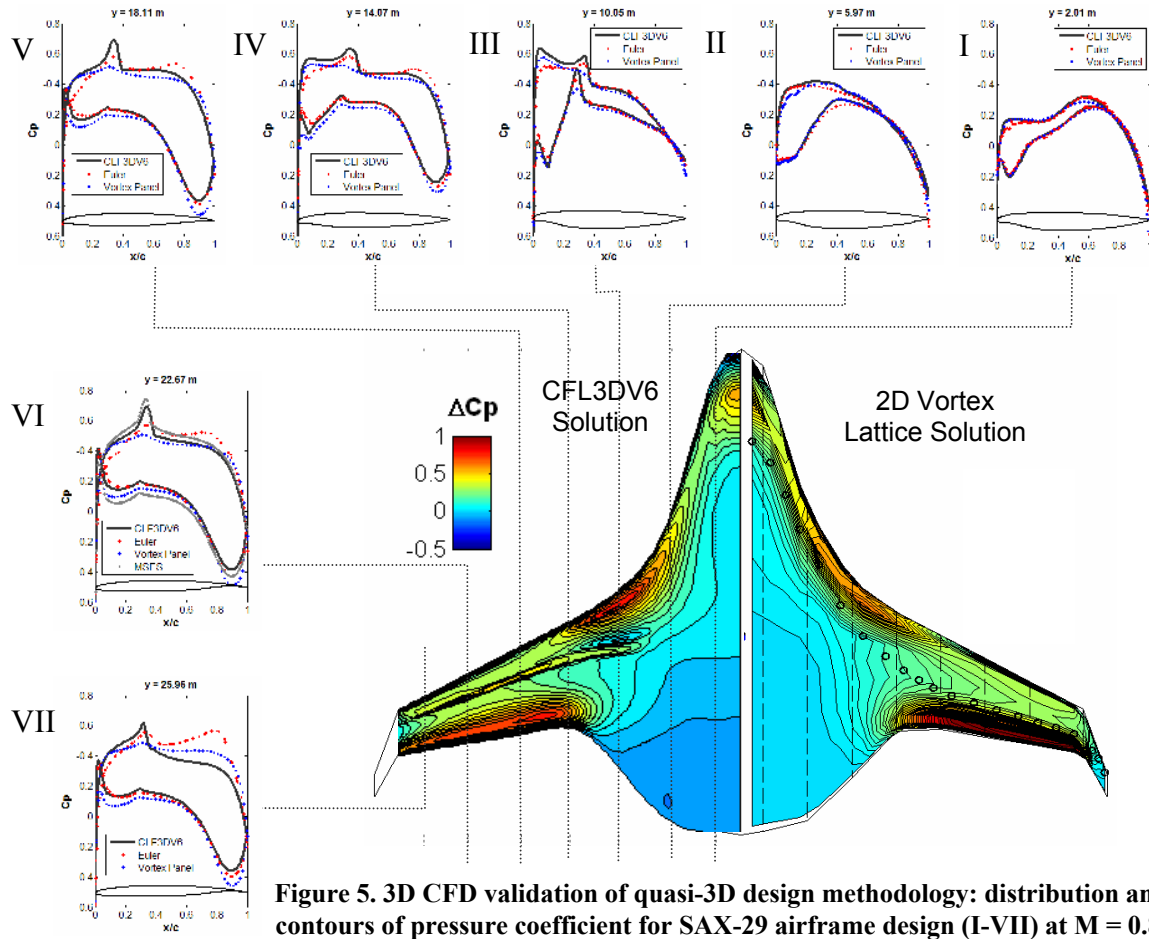


Figure 5. 3D CFD validation of quasi-3D design methodology: distribution and contours of pressure coefficient for SAX-29 airframe design (I-VII) at $M = 0.8$.

capturing the three-dimensionality of the viscous flow over the centerbody. A three-dimensional Navier Stokes CFD analysis of the SAX-29 planform using the CFL3DV6 code was conducted at Boeing Phantom Works. The assessment showed that the quasi-3D design methodology is capable of capturing the major aerodynamic features and over predicts ML/D by 13% relative to the CFL3DV6 solution. The validation demonstrates that the quasi-3D design methodology is adequate for optimization purposes where a rapid turnaround time is required. At the end of the optimization process, a fully viscous three-dimensional calculation is suggested to evaluate the final design.

CFL3D²³ is a Navier-Stokes CFD code developed at NASA Langley Research Center for solving 2-D or 3-D flows on structured grids. The solution relied on the Spalart-Allmaras turbulence model and incorporated nearly 4 million grid cells. The analysis was conducted without winglets and computations were conducted for flight Mach numbers ranging from 0.5 to 0.85 at angles of attack between 2.5 and 5.5°.

The aerodynamic loading characteristics of the SAX-29 airframe design are outlined in Figure 5 for a cruise Mach number of 0.8. The loading contours from the two-dimensional vortex lattice code are qualitatively similar to the three-dimensional Navier Stokes solution. Both solutions capture the centerbody loading due to the aerodynamic shaping of the leading edge region, the centerbody-wing junction loading, and the aft loading on the supercritical outer wing sections. The solutions differ in the weak shock that forms on the outer wings. This is because the two-dimensional vortex lattice solution cannot capture shock waves and compressibility effects are modeled with a Prandtl-Glauert correction. In the CFL3DV6 computation the outer wing shock is augmented by the presence of boundary layers which are not captured by the Euler or vortex panel solutions. To capture the outer wing shock in the quasi-3D design methodology, two-dimensional viscous, compressible airfoil calculations (MSES) are carried out on swept airfoil sections. An example is shown in subplot VI where the MSES solution is marked in grey. In the developed methodology, the outer wing loading is estimated by the two-dimensional vortex lattice code and used to set the loading in the sectional viscous airfoil analysis (MSES). This approach breaks down for the highly three-

dimensional flow near the centerbody (comparison not shown). Based on this assessment, inviscid three-dimensional vortex panel solutions were generated for all subsequent designs to evaluate the aerodynamic loading.

The CFL3DV6 results for SAX-29 are shown in Figure 6 and yield an ML/D of 16.7 at the begin cruise lift coefficient of 0.197. The maximum ML/D of 17.3 occurs at a lift coefficient of 0.254. At the begin cruise lift coefficient, the quasi-3D design methodology over predicts the CFL3DV6 estimate by 13%, which corresponds to a drag difference of 0.0011. The discrepancy is due to the simplifications made in the developed methodology. To estimate the viscous drag on the centerbody, the quasi-3D design methodology relies on empirical drag estimates for bodies of revolution at high Reynolds number reported by Hoerner.²⁴ Furthermore the CFL3DV6 calculations indicate that the SAX-29 airframe has the potential to achieve a maximum ML/D of 17.3 by operating at a higher cruise Mach number of 0.83 (not shown in Figure 6).

In summary the developed quasi-3D design methodology adequately captures the three-dimensional aerodynamic features and performance for optimization purposes. Based on the above assessment, the centerbody planform shape and airfoil profiles of the SAX-29 design were frozen in further design optimizations. Although mid and outer wing airfoil profiles could have been redesigned to eliminate the weak shock on the outer wing, the profiles were deemed acceptable in the light of the relatively short project timeframe and the potentially small performance gains to be made.

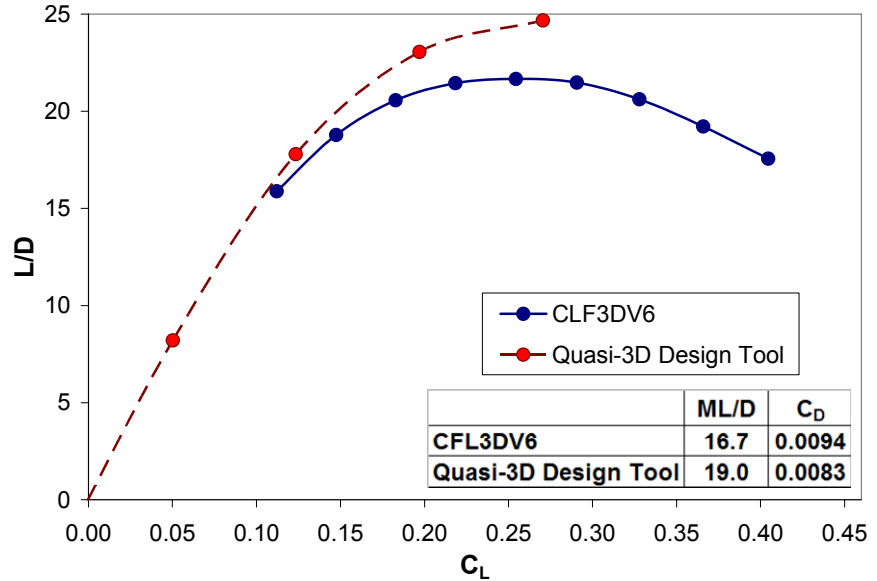


Figure 6. Comparison of SAX-29 performance estimates at $M = 0.8$: quasi-3D design methodology (red) and CFL3DV6 calculation (blue).

VI. SAX-40 Aircraft Design

The SAX-40 conceptual aircraft design, shown in Figure 1, was created based on the SAX-29 centerbody and airfoils while the outer wing planform and twist were optimized for low approach noise and high fuel efficiency at cruise. This section presents the aircraft design with emphasis on the design strategies and their implications.

A. Overall Performance

The geometry and performance of SAX-40 are given in Tables 1 and 2. The airfoil stack, planform shape, and distributions of twist and thickness are presented in Figure 7. Unshaded areas within the top-down view of planform have airfoil profiles that are interpolated from neighboring sections. Using the quasi-3D design methodology, the ML/D is calculated to be 20.1 at beginning of cruise. Due to time constraints a fully viscous three-dimensional CFD analysis of SAX-40 could not be conducted. If the ML/D is over predicted by 13% as discussed above for SAX-29, the ML/D at begin cruise would reduce to 17.5. In comparison, an ML/D of 18 is reported for the BWB design by Liebeck,⁴ 15.5 for the Boeing 777,²⁵ and 13.4 for the BWB by Qin et al.²⁶

As illustrated by the planform comparison in Figure 3, the optimizer redistributed the wing area by removing chord from the mid wing region at a spanwise location of about 40 ft and by increasing the overall wing span. This led to a 6% increase in ML/D between SAX-29 and SAX-40. The elliptical lift distribution resulting from this area redistribution and outer wing optimization is shown in Figure 8.

Parameter	Value
Wing area, ft ²	8,998
Wing span, ft	207.4
Cruise Mach	0.8
Outer-Wing Twist, °	-3.25
Stall Speed, knots	96.0

	Begin Cruise	End Cruise
Cruise Altitude, ft	40,000	45,000
Lift Coefficient	0.2064	0.2091
Angle of Attack, deg	2.7	2.7
C.G., % centerbody chord	58.3	57.1
Static Margin, % / in	5.9 / 31	9.5 / 50
Elevator Deflection, deg	0	0
Thrust Vector Angle, deg	0	10.5 up
ML/D	20.1	18.8

Table 1. SAX-40 geometric and aerodynamic performance parameters.

Coefficient	Value
C_L	0.2064
C_D	0.0082
C_{Di}	0.0024
C_{Dp}	0.0009
C_{Dp} centerbody	0.0004
C_{Dp} wing	0.0005
C_{Df}	0.0045
C_{Df} centerbody	0.0027
C_{Df} wing	0.0018
C_D wave	0.0001
$C_{D,engine}$ nacelles	0.0004

Table 2. SAX-40 lift, moment and drag coefficients at beginning of cruise.

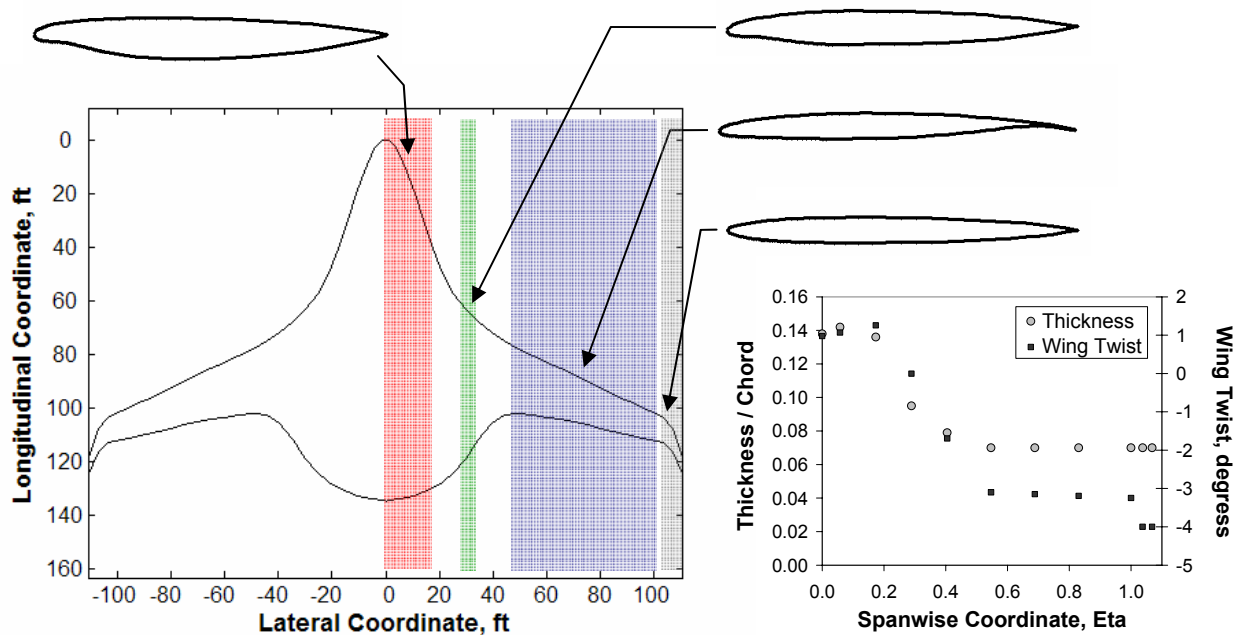


Figure 7: SAX-40 airfoil sections, planform shape, and distributions of twist and airfoil thickness.

B. Weight and Balance

The aircraft weight buildup, presented in Table 3, includes a design payload for 215 passengers at 240 lbs per passenger, 20 lbs per passenger heavier than mandated by FAA AC120-27E.²⁷ At 220 lbs/passenger the aircraft could carry 236 passengers which has ramifications in terms of estimated fuel burn. More details are given later in this section.

One of the challenges inherent in scaling the SAX and other all-lifting body airframe designs to shorter range or smaller payload is the high empty weight fraction, OEW over MTOW. In the Breguet range equation the empty weight fraction, along with ML/D and specific fuel consumption, determine the aircraft fuel burn. The SAX-40 weight fraction of 0.62 is higher in comparison to conventional aircraft configurations. For example the Boeing 767-300 introduced in 1982, an aircraft with a similar mission to the SAX-40, has a weight fraction of 0.52.²⁵

Component	Weight, lbs
Maximum Take-Off Weight, MTOW	332,560
Operating Empty Weight, OEW	207,660
Design Payload	51,600
Fuel with reserves	73,310
Structure	104,870
Fixed Equipment	51,220
Landing Gear	14,760
Propulsion	36,810

Table 3. SAX-40 aircraft weight buildup.

C. Internal Layout

The internal configuration of the aircraft design is presented from three views in Figure 8. The interior of the SAX-40 cabin was not designed in detail but the outer cabin shape was used as a constraint in the planform and airfoil design optimization. More specifically, the outer skin was required to enclose the passenger cabin and the spar box. The original cabin dimensions were set by WingMOD which then grew as the planform area increased by incorporating the aerodynamic shaping of the centerbody leading edge. The SAX-40 cabin has 2,570 ft² (239 m²) of floor area. With 215 passengers, the cabin passenger density is 0.9 passengers/m². In comparison, the Boeing 767-300 and 767-400 have passenger densities of 1.4 passengers/m² in a dual class configuration.²⁸ The SAX-40 cabin could thus carry 335 passengers at this density. The cabin was defined as a box with a height of 6.6 ft, but as shown in the side view of Figure 8, there is much space between the cabin top and aircraft skin such that the cabin height could be increased up to 9.7 ft.

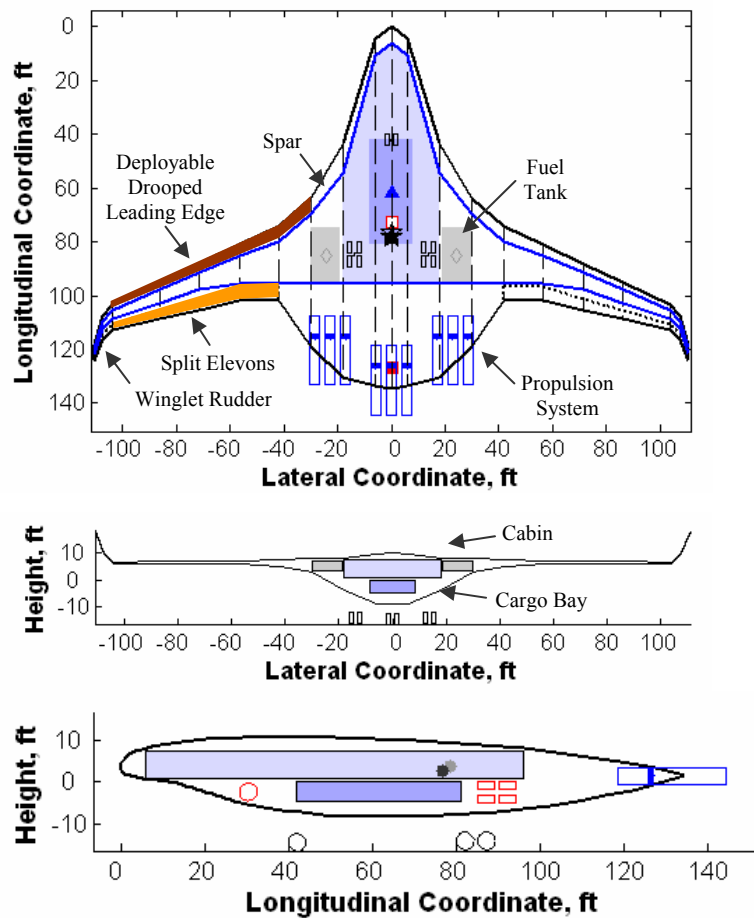


Figure 8. Internal layout illustrating cabin, cargo, fuel tanks, spars, propulsion system, and undercarriage.

The SAX-40 cargo bay was set at 39.4 x 16.4 x 4.6 ft (volume of 2,970 ft³). The fuel tank capacity of 12,000 gal (80,000 lb) is provided via two inner wing tanks close to the aircraft center of gravity. Fuel pumping is not necessary to maintain static stability. The planform has considerable empty space in the wings that can potentially be used to carry additional fuel for increased range. This additional fuel however would lead to a larger thrust requirement on take-off which in turn would increase noise. The faired, dual four-wheel main gear bogeys are stowed behind the cargo bay while the simple dual wheel nose gear retracts forward into the fuselage. The embedded propulsion system is shown to scale in the figures and the engine fan faces are marked to indicate the inlet duct length.

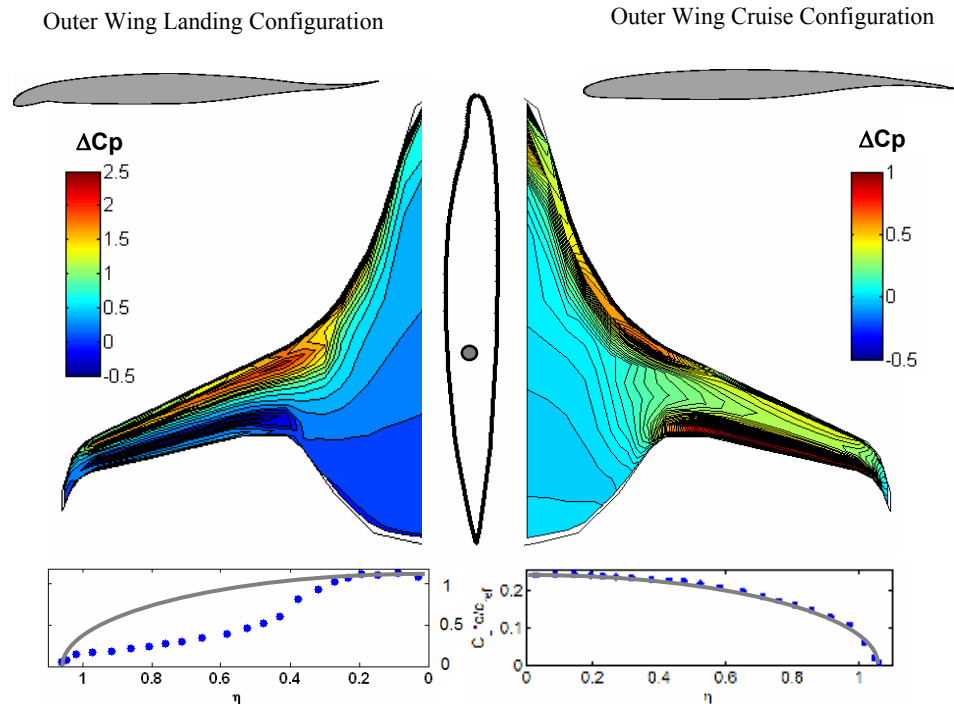


Figure 9. Two-dimensional vortex lattice estimate of airframe loading distribution during cruise and approach / landing.

D. Pitch Trim and Static Stability

The outer wing profile configuration and loading distribution obtained from the two-dimensional vortex lattice solution for approach and cruise conditions are shown in Figure 9. For reference, the centerbody profile is shown to scale and the dot indicates the aircraft center of gravity. The supercritical airfoils on the outer wing are twisted 3.5° outwash such that at beginning of cruise the outer wing loading is concentrated aft of the aircraft center of gravity. This loading is naturally balanced by the lift generated in the forward region of the centerbody. As fuel is burned from begin to end of cruise, the thrust angle is increased for pitch trim. A maximum thrust vectoring angle of 10.5° is reached at the end of cruise. Thrust vectoring is preferred over deflecting elevators in order to keep the cabin angle below 3°. Elevator deflections for pitch trim unload the outer wings such that the aircraft angle of attack has to increase to maintain steady flight.

At begin cruise a positive 5.9% static margin is estimated using the two-dimensional vortex lattice solution. This corresponds to a distance between center of gravity and center of pressure of 31 inches which exceeds the expected 25 inch travel of the passenger and cargo center of gravity.³⁰ As fuel is burned during cruise, the center of gravity moves forward and the static margin increases to 9.5% equivalent to 50 inches. In comparison, the BWB reported in Liebeck⁴ has a positive static margin of 5% while trimmed at cruise.

The SAX-40 suction and pressure surface C_p distributions from the vortex panel solution are plotted in Figure 10. The loading due to the aerodynamic shaping of the centerbody leading edge is evident in the increased pressure coefficient in the forward region. The centerbody airfoil design has minimal aft camber in order to avoid an untrimmable nose-down moment. This also results in an enhanced external pre-compression of the flow upstream of the engine inlets mitigating the aerodynamic challenge of integrating the propulsion system into the airframe. A detailed discussion of the engine integration and inlet design can be found in Plas et al.⁶

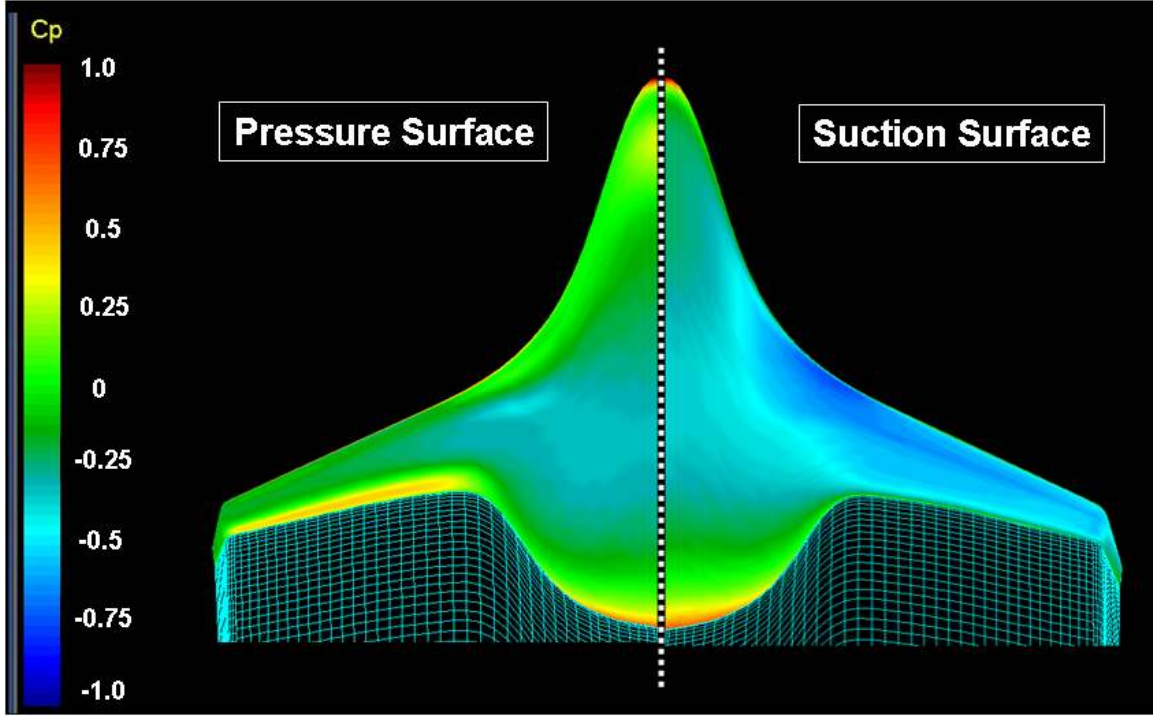


Figure 10. Pressure distribution at Mach 0.8 estimated with three-dimensional vortex panel method.

E. Low Speed Capability

The change in planform depicted in Figure 3 resulted in a decrease in stall speed from 118 knots (63.8 m/s) for SAX-12 to 96.0 knots (49.4 m/s) for SAX-40. The stall speeds were estimated at the nominal landing weight which includes the design payload and the reserve fuel. For comparison, aircraft of similar weight to SAX-40 have typical stall speeds of 114 to 130 knots which corresponds to approach speeds of 140 to 160 knots.³ According to FAR25.125,³¹ the approach speed must exceed 1.23 times the stall speed. The stall speed can be reduced by decreasing the sweep angle, Λ , but this also incurs a cruise wave drag penalty. The tradeoffs are examined via infinite swept wing theory, in which the flow in the airfoil plane normal to the spanwise axis sees a reduced Mach number, M , and a reduced dynamic pressure, q :

$$M_{\perp} = M \cos(\Lambda) \quad (1)$$

$$q_{\perp} = q \cos^2(\Lambda) \quad (2)$$

The resulting perpendicular 2-D airfoil coefficients $c_{l,max}$ and $c_{d,pressure}$ then give the 3-D aircraft coefficients as follows:

$$C_{L,max} = c_{l,max} \cos^2(\Lambda) \quad (3)$$

$$C_{D,pressure} = c_{d,pressure} \cos^3(\Lambda) \quad (4)$$

These quantify the effect of the sweep angle Λ on $C_{L,max}$ and hence the stall speed, and also on the wave drag which is a part of $C_{D,pressure}$. In the optimization, a compromise between cruise performance and stall speed is reached at a mid-chord sweep of 19° .

During approach and in low speed flight, the SAX-40 aircraft is trimmed by combining thrust vectoring and elevon deflections. Downward vectored idle thrust at 30° and simultaneously upward deflected elevons at 18.5° unload the outer wing trailing edge region and require a large angle of attack to generate the necessary lift. A drooped leading edge is implemented to achieve an angle of attack of 15.6° . A detailed assessment of the high-lift system can be found in Andreou et al.³² The experimental study demonstrates that the noise radiated from drooped leading edges is comparable to the levels of airfoil self-noise. The consequence of the high angle of attack

configuration is a non-elliptic lift distribution generating sufficient induced drag to trim the aircraft on a 3.9° flight path angle. To demonstrate glide slope capture at a 6° flight path angle necessary for certification, split elevons act as drag rudders in non-silent operation.

The SAX-40 airframe was designed for low stall speed to reduce the airframe noise on approach. This inherently leads to enhanced low speed performance during take-off. At take-off thrust vectoring is used for pitch trim since elevon deflections decrease the aircraft L/D and deteriorate the climb-out performance.² To rotate the aircraft at take-off the elevons are deflected in combination with vectored thrust.²²

	Fuel Economy, Passenger-Miles per Gallon
SAX-40	~124
Toyota Prius Hybrid Car	120 with 2 people
Boeing 777	86 to 101
Airbus A320	79 to 97
Boeing 707	46 to 58

Table 4. Calculated fuel economy for SAX-40 in comparison with the Toyota Prius hybrid electric car³³ and existing aircraft.²⁵

F. Fuel Efficiency

The SAX-40 aircraft design has the potential for large reductions in fuel burn. A fuel burn of 124 passenger-miles per gallon is calculated and compared to airline operational data as compiled by Lee et al.²⁵ in Table 4. All of the existing aircraft data is for 220 lbs/passenger whereas the SAX-40 fuel burn calculation assumed 215 passengers at 240 lbs/passenger. A further improvement in fuel economy could be achieved if 236 passengers are assumed at the standard weight of 220 lbs/passenger. The SAX-40 fuel burn estimate is based on a specific fuel consumption of 0.49 lb/lb*hr, which includes the effect of boundary layer ingestion. A detailed discussion of propulsion system performance for this highly integrated configuration can be found in de la Rosa Blanca et al.⁹ and Plas et al.⁶.

G. Aircraft Noise

The aircraft approach velocity for SAX-40 is calculated to be 28% lower than the typical approach velocity for similar sized aircraft. This improvement in low speed flight capability contributes significantly to the overall reduction in noise: the calculated noise level at the airport perimeter of 63 dBA is near the background noise of a well-populated area. As shown in Figure 12 and discussed at length in two companion papers focused on the assessment of take-off noise² and approach noise,³ a reduction in cumulative noise (sideline, take-off and approach) of 75 cumulative EPNdB is estimated relative to the ICAO Chapter 4 requirement of 284.5 cumulative EPNdB. The effective perceived noise levels (EPNdB) were computed according to the FAA procedures documented in Part 36.³⁴ Tone corrections were neglected since tonal noise could not be computed for the airframe noise sources.

VII. Conclusion and Outlook

A quasi-3D design methodology was developed for the conceptual design of an aircraft with step changes in noise reduction and fuel efficiency. The design methodology was validated using a fully viscous, three-dimensional CFD calculation and was subsequently used in an

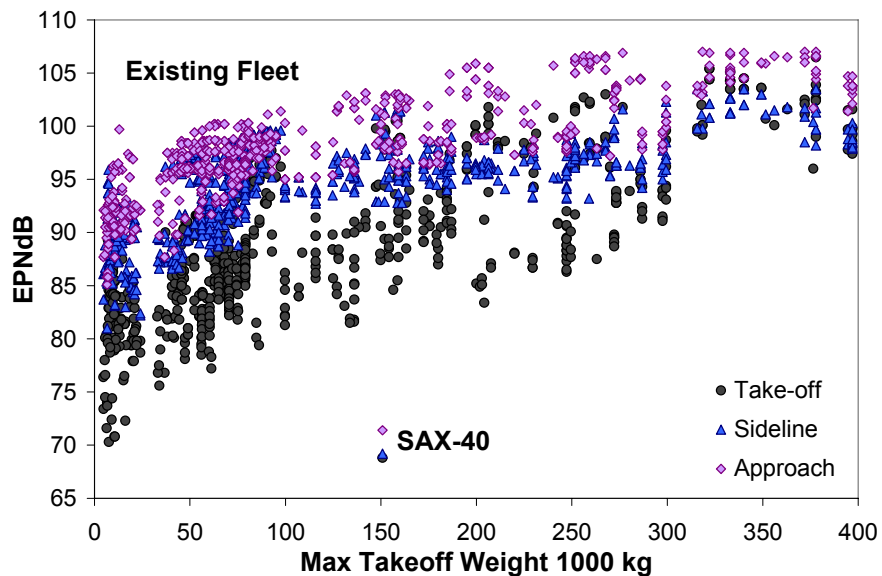


Figure 12. Estimated EPNL for the SAX-40 aircraft with the Granta-3401 propulsion system in comparison to U.S. certified jet powered airplanes.³⁵

aircraft design optimization framework. The key feature of the resulting aircraft design, SAX-40, is the aerodynamically shaped leading edge of the airframe centerbody. The all-lifting airframe is optimized to generate a lift distribution that balances aerodynamic moments for pitch trim and static stability, achieves an elliptical span load on cruise, and increases the induced drag on approach reducing the stall speed.

The conceptual aircraft design yields a cruise ML/D of 20.1 and a potential fuel burn of 124 pax-miles per gallon. The trimmed approach speed is calculated to be 28% lower than existing commercial aircraft, enabling a step change in airframe noise reduction. The estimated maximum noise level at the airport perimeter is 62 dBA, which corresponds to a computed 75 cumulative EPNdB reduction relative to the ICAO Chapter 4 requirements. The economic analysis of a silent aircraft are presented in a companion paper.³⁶

Some of the technologies introduced yield a number of technical challenges and are of considerable risk. These must be overcome before this design concept can become a reality. For example the pressure vessel and structural integrity of the unconventional all-lifting body pose challenges in fabrication and manufacturing. The low-speed aerodynamics of the airframe need to be assessed using three-dimensional viscous flow computations and the stowage and implementation of a faired undercarriage need to be further analyzed. A major challenge is the integration of the distributed propulsion system in the airframe. Inlet distortion noise and forced vibration issues due to non-uniform inlet flow must be resolved and the mechanical challenges of the geared fan transmission system and the variable area thrust vectoring exhaust nozzles must be overcome.

In summary, the SAX-40 conceptual aircraft design meets the objectives of a “silent” and fuel efficient aircraft, given the high risk of the technologies used.

Acknowledgments

Without the experience and encouragement of Bob Liebeck, Dino Roman, and Sean Wakayama at Boeing Phantom Works, the aircraft design presented in this paper could not have been achieved. Their continuous support and the CFL3DV6 analysis conducted by Dino Roman are gratefully acknowledged. The authors are also indebted to many members of the Silent Aircraft Initiative who have been instrumental to the completion of this work. Special thanks go to Dan Crichton for conducting the take-off EPNL calculations, Steven Thomas for providing the renderings of the aircraft designs, Anya Jones for her extensive work in setting up the weights model and improving the logic behind the design codes, and Professor Karen Willcox for her assistance in the area of blended-wing-body type design and optimization. This research was funded by the Cambridge-MIT Institute which is gratefully acknowledged. Matthew Sargeant is grateful to the Cambridge Australia Trust for his doctoral fellowship.

References

1. Manneville, A., Pilczner, D., and Spakovszky, Z., “Preliminary Evaluation of Noise Reduction Approaches for a Functionally Silent Aircraft,” *AIAA Journal*, Vol. 43, No. 3, pp. 836-840, 2006.
2. Crichton, D. de la Rosa Blanco, E., Law, T., and Hileman, J. “Design and operation for ultra low noise take-off,” AIAA Paper 2007-0456, 2007.
3. Hileman, J. I., Reynolds, T. R., de la Rosa Blanco, E., and Law, T., “Development of Approach Procedures for Silent Aircraft,” AIAA Paper 2007-0451, 2007.
4. Liebeck, R.L., “Design of the Blended-Wing-Body Subsonic Transport,” *Journal of Aircraft*, Vol. 41, No. 1, pp. 10-25, 2004.
5. Diedrich, A., Hileman, J., Tan, D., Willcox, K., Spakovszky, Z. “Multidisciplinary Design and Optimization of the Silent Aircraft,” AIAA Paper 2006-1323, 2006.
6. Plas, A. P., Madani, V., Sargeant, M. A., Greitzer, E. M., Hall, C. A., Hynes, T. P., “Performance of a Boundary Layer Ingesting Propulsion System,” AIAA Paper 2007-0450, 2007.
7. Hall, C. A. and Crichton, D., “Engine and Installation Configurations for a Silent Aircraft,” ISABE-2005-1164, 2005.
8. Hall, C. A. and Crichton, D., “Engine Design Studies for a Silent Aircraft,” GT2006-90559, presented at the ASME Turbo Expo, Barcelona, May 2006.
9. de la Rosa Blanca, E., Hall, C., and Crichton, D., “Challenges in the Silent Aircraft Engine Design,” AIAA Paper 2007-0454, 2007.
10. Agarwal, A., and Dowling, A., “A Ray Tracing Approach to Calculate Acoustic Shielding by the Silent Aircraft Airframe,” AIAA Paper 2006-2618, 2006.
11. Law, T., and Dowling, A., “Optimization of Traditional and Blown Liners for a Silent Aircraft” AIAA Paper 2006-2525, 2006.
12. Qualye, A., Dowling, A., Babinsky, H., Graham, W., Sijtsma, P., “Landing Gear for a Silent Aircraft,” AIAA Paper 2007-0231, 2007.

- ^{13.} Jaeger, S.M., Burnside, N.J., Soderman, P.T., Horne, W.C., and James, K.D., "Microphone Array Assessment of an Isolated 26%-Scale, High-Fidelity Landing Gear," AIAA Paper 2002-2410, 2002.
- ^{14.} Sakaliyski, K. D., Hileman, J. I., and Spakovszky, Z. S., "Aero-acoustics of Perforated Drag Plates for Quiet Transport Aircraft," AIAA Paper 2007-1032, 2007.
- ^{15.} Shah, P., Mobed, D., and Spakovszky, Z. S., "Engine Air-Brakes for Quiet Transport Aircraft", AIAA Paper 2007-1033, 2007.
- ^{16.} Lilley, G.M., "The Prediction of Airframe Noise and Comparison with Experiment," *Journal of Sound and Vibration*, Vol. 239, Issue 4, pp. 849-859, 2001
- ^{17.} Herr, M., and Dobrzyinski, W., "Experimental Investigations in Low-Noise Trailing-Edge Design," *AIAA Journal*, Vol. 43, No. 6, pp. 1167-1175, 2005.
- ^{18.} Lockard, D.P. and Lilley, G.M., "The Airframe Noise Reduction Challenge," NASA TM-2004-213013, 2004.
- ^{19.} Wakayama, S., "Blended-wing-body optimization problem setup" AIAA Paper 2000-4740, 2000.
- ^{20.} Hileman, J. I., Spakovszky, Z. S., Drela, M. and Sargeant, M., "Aerodynamic and Aeroacoustic Three-Dimensional Design for a "Silent" Aircraft," AIAA paper 2006-0241, 2006.
- ^{21.} Wakayama, S., and Kroo, I., "Subsonic Wing Planform Design Using Multidisciplinary Optimization," *AIAA Journal*, Vol. 32, No. 4, pp. 746-753, 1995.
- ^{22.} Thomas, S. and Dowling, A., "A Dynamical Model and Controller for the Silent Aircraft," AIAA Paper 2007-0866, 2007.
- ^{23.} Rumsey, C.L., "CFL3D Version 6.4 Home Page," <http://cfl3d.larc.nasa.gov/Cfl3dv6/cfl3dv6.html>, August 31, 2006.
- ^{24.} Hoerner, S.F., *Fluid Dynamic Drag*. Published by the author, 1965.
- ^{25.} Lee, J.J., Lukachko, S.P., Waitz, I.A. and Schafer, A., "Historical and Future Trends in Aircraft Performance, Cost and Emissions," *Annu. Rev. Energy Environ.*, Vol. 26, pp. 167-200, 2001.
- ^{26.} Qin, N., Vavalle, A., Le Moigne, A., Laban, M., Hackett, K., and Weinerfelt, P., "Aerodynamic Considerations of Blended-Wing-Body Aircraft," *Prog. Aero. Sciences*, Vol. 40, pp. 321-343, 2004.
- ^{27.} Federal Aviation Administration, "Aircraft Weight and Balance Control," Advisory Circular AC120-27E, Chapter 2, Section 2. June 2005.
- ^{28.} Boeing Commercial Airplanes Group, "767-400ER Airplane Characteristics for Airport Planning," 2000.
- ^{29.} Wakayama, S. Personal Communication on Cabin Angle, Dec 2006.
- ^{30.} Boeing Seattle Personal Communication on Center of Gravity Travel, May 31 2006.
- ^{31.} Federal Aviation Administration, "Part 25 Airworthiness Standards: Transport Category Airplanes, Landing," Federal Aviation Regulation Sect.25.125, 2002.
- ^{32.} Andreou, C., Graham, W., and Shin, H.-C., "Aeroacoustic Study of Airfoil Leading Edge High-Lift Devices," AIAA Paper 2006-2515, 2006.
- ^{33.} Toyota Motors Sales, USA, "Toyota Prius Specifications," <http://www.toyota.com/prius/specs.html>, 2005.
- ^{34.} Federal Aviation Administration, "Part 36—Noise Standards: Aircraft Type and Airworthiness Certification," Electronic Code of Federal Regulations (e-CFR) Title 14, Chapter 1, Subchapter C, Part 36, Nov 2006.
- ^{35.} Federal Aviation Administration, "Noise Levels for U.S. Certificated and Foreign Aircraft. Appendix 1 - U.S. Certificated Turbojet Powered Airplanes," AC36-1H, http://www.faa.gov/about/office_org/headquarters_offices/aep/noise_levels/, Nov. 2001.
- ^{36.} Tam, R., Belobaba, P., Polenske, K. R., and Waitz, I. "Assessment of Silent Aircraft-Enabled Regional Development and Airline Economics in the UK," AIAA Paper 2007-455, 2007.